JACS
JOURNAL OF THE AMERICAN CHEMICAL SOCIETY

COMMUNICATION

pubs.acs.org/JACS

# Bidirectional and Unidirectional PCET in a Molecular Model of a Cobalt-Based Oxygen-Evolving Catalyst

Mark D. Symes, Yogesh Surendranath, Daniel A. Lutterman, and Daniel G. Nocera*

Department of Chemistry, Massachusetts Institute of Technology, Cambridge, Massachusetts 02139-4307, United States

Supporting Information

**ABSTRACT:** The oxidation of water to molecular oxygen is a kinetically demanding reaction that requires efficient coupling of proton and electron transfer. The key proton-coupled electron transfer (PCET) event in water oxidation mediated by a cobalt-phosphate-based heterogeneous catalyst is the one-electron, one-proton conversion of $Co^{III}$—OH to $Co^{IV}$—O. We now isolate the kinetics of this PCET step in a molecular $Co_4O_4$ cubane model compound. Detailed electrochemical, stopped-flow, and NMR studies of the $Co^{III}$—OH to $Co^{IV}$—O reaction reveal distinct mechanisms for the unidirectional PCET self-exchange reaction and the corresponding bidirectional PCET. A stepwise mechanism, with rate-limiting electron transfer is observed for the bidirectional PCET at an electrode surface and in solution, whereas a concerted proton—electron transfer displaying a moderate KIE (4.3 ± 0.2), is observed for the unidirectional self-exchange reaction.

As global demand for energy continues to grow, the need to find a carbon-neutral and sustainable energy source for future generations has become imperative.[1−4] An especially attractive solution is to store solar energy in the form of chemical bonds via the electrochemical splitting of water to produce hydrogen and oxygen.[5−7] In this process, the electrochemical oxidation of water to $O_2$ is the bottleneck because it is a kinetically demanding four electron—four proton transformation. The intimate coupling of electron and proton transfer[8−11] thus becomes a key requirement for effecting the solar fuels process of water splitting.

We recently reported a heterogeneous Co-Pi catalyst[12] that forms spontaneously upon electrolysis of Co(II) in phosphate-buffered solutions at neutral pH.[13] This catalyst enhances the efficiency of electrochemical and photoelectrochemical water oxidation and is of interest because it (1) forms in situ under mild conditions on a variety of conductive substrates from inexpensive and earth-abundant materials;[13,14] (2) exhibits high activity in natural water and seawater at room temperature;[15] (3) is self-healing by reversing catalyst corrosion at open circuit upon reapplication of an anodic potential;[16] (4) can be interfaced with light-absorbing and charge-separating materials to enhance photoelectrochemical water splitting;[17−19] and (5) is a functional and related structural model of the oxygen-evolving complex of Photosystem II (PS II).[20] With regard to the latter, XAS studies[21,22] have established that the Co-Pi is a structural relative of the oxygen-evolving complex (OEC) of PSII. Shown in Scheme 1 are the structures of the PSII OEC[23] and the core structure of Co-Pi as deduced from XAS where a distribution of cluster sizes is observed, where the seven-atom cluster shown in Scheme 1 predominates in ca. nanometer thin films of the catalyst. Both systems have a partial cubane. In the OEC, the cube is completed with a $Ca^{2+}$ ion; although the alkali metal ions for Co-Pi have not been located, they likely reside on the three-fold oxygen triangle to complete the cube structure, as is the case for cobaltates.[24] As highlighted in Scheme 1, Co-Pi is the corner-sharing head-to-tail dimer of the OEC monomer of PSII. The metal—metal ($d$ = 2.8 Å) and metal—oxo ($d$ = 1.9 Å) distances in Co-Pi and PSII OEC are similar. Thus, model cubane systems not only shed light on the PCET water activation chemistry of Co-Pi but may also provide insight into the mechanism of PSII OEC.

**Scheme 1**

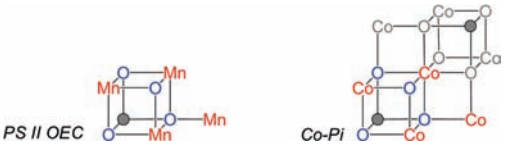


XANES[22], EPR[25] and electrochemical studies[26] of Co-Pi have, together, established the proton-coupled electron transfer (PCET) conversion of $Co^{III}$—OH to $Co^{IV}$—O as a key mechanistic step prior to $O_2$ evolution. The same conversion is also believed to be critical to Co-oxide-mediated water oxidation in alkaline media.[27−29] Herein, we isolate the kinetics of this key step in a $Co_4(\mu_3\text{-O})_4$ molecular model cubane, $[Co_4O_4(CO_2Me)_2(bpy)_4](ClO_4)_2$ (**1**), originally reported by Christou and co-workers[30] (Figure 1), which is a structural relative of Co-Pi with complete Co residency within the cube. In both Co-Pi and this molecular model, $\mu_3$-O/OH moieties link the Co centers. We now report electrochemical, stopped-flow, and NMR-based studies of the $Co^{III}$—OH to $Co^{IV}$—O conversion in **1** that reveal that the PCET reaction for which electron and proton are transferred to the same molecule (unidirectional) is a concerted PCET, whereas transfer of the proton and electron to different molecules (bidirectional) occurs by stepwise PCET.

The stepwise and concerted PCET pathways of the cubane model system are detailed in Figure 1. As synthesized, all Co centers in the cubane, **1**, are in the $3^+$ oxidation state, and the cluster can be protonated to yield **1**-$H^+$, which exhibits a p$K_a$ of 3.15.[31] The cyclic voltammogram (CV) of **1** at pH > 4 exhibits a reversible one-electron oxidation[32] with an $E_{1/2}$ = +1.25 V (all potentials are reported vs the normal hydrogen electrode). This potential is similar to the potentials (>+1.1 V) at which Co(IV) is detected in Co-Pi.[25] Thus, the

**Received:** December 10, 2010
**Published:** March 17, 2011

ACS Publications © 2011 American Chemical Society



dx.doi.org/10.1021/ja110908v | J. Am. Chem. Soc. 2011, 133, 5174–5177

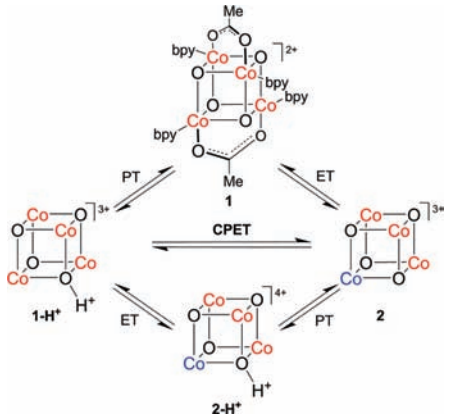


**Figure 1.** Potential PCET mechanisms for the molecular model cubane. We note that charge is delocalized within the cube;[32] depiction of Co(III) centers (red) and Co(IV) center (blue) is solely for illustrative purposes. At pH < 3.1, the protonated form of the cubane, **1**-$H^+$, is the stable species. At pH > 3.1, the cubane is deprotonated, and **1** is the stable species.

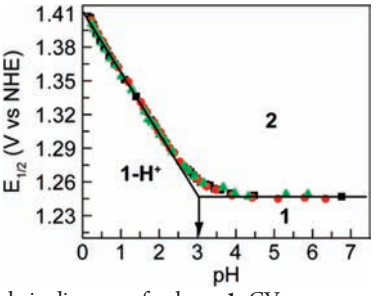


**Figure 2.** Pourbaix diagram of cubane **1**. CV scans recorded at a scan rate of 0.1 V $s^{-1}$. The green, black, and red points correspond to three separate sets of data. Labels on the plot indicate zones of thermodynamic stability for **1**, **1**-$H^+$, and **2**.

structural and electrochemical similarities of the model led us to investigate potential PCET reactions from **1**-$H^+$.

To establish the proton and electron dependencies of the Co(III)-to-Co(IV) conversion over a wide pH range, a Pourbaix diagram (pH vs $E_{1/2}$) was constructed (Figure 2). At low pH (<2) a straight line is obtained with a slope of −55 mV/pH unit, which is in close agreement with the slope (−59 mV/pH unit) predicted by the Nernst equation for a one-electron, one-proton redox process. The data are consistent with the concomitant removal of the only proton on the cubane core from **1**-$H^+$ upon one-electron oxidation over the pH range $0 \le$ pH < 4. As shown in Figure 2, the formal potential of the redox process becomes invariant with pH > 4, indicating that the cubane is in its fully deprotonated form (**1**) and that a simple one-electron transfer reaction prevails. We note that a second plateau region at lower pH and higher $E_{1/2}$ would indicate a pH/potential regime in which the oxidized cubane remained protonated as **2**-$H^+$. No such plateau was observed in this study (pH ≥ 0). Extrapolation of the low and high pH data of Figure 2 to their point of intersection yields the p$K_a$ of the reduced species in this electrochemical equilibrium, which is found to be ~3.1 from Figure 2. This value compares favorably to the value of 3.15 obtained by titration of **1**-$H^+$ with NaOH.[31]

To probe the kinetics of the redox processes of Figure 2, the scan-rate dependence of the CVs of **1** and **1**-$H^+$ was monitored. As scan rate is increased, the splitting of anodic and cathodic peak potentials increases (Figure 3a), allowing the construction of "trumpet plots".[33] The rate constant for the oxidation of the cubane, $k$, can be extracted from these trumpet plots by fitting the

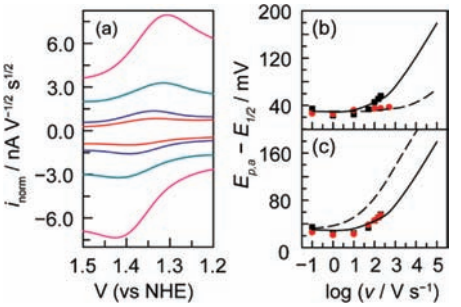


**Figure 3.** (a) Overlay of representative normalized ($i_{norm} = i/\nu^{1/2}$) CVs taken of a 0.5 mM solution of **1**-$H^+$ in 0.1 M $H_2SO_4$/0.2 M $KNO_3$ at 1 (red), 10 (blue), 100 (teal), and 200 V/s (pink) using a glassy carbon microelectrode. (Right) Difference between anodic peak potential and midpoint potential ($E_{p,a} - E_{1/2}$) vs log of scan rate. (b) Comparison between pH 1 (■) and pH 4 (red ●). Simulated curves are plotted for $k$ = 0.17 (—) and 2 cm $s^{-1}$ (- - -). (c) Comparison between 0.1 M $H_2SO_4$/0.2 M $KNO_3$ in $H_2O$ (■) and 0.1 M $D_2SO_4$/0.2 M $KNO_3$ in $D_2O$ (red ●). Simulated curves are plotted for $k$ = 0.17 (—) and 0.041 cm $s^{-1}$ (- - -). The latter rate constant is consistent with $^1$H NMR measurements (vide infra).

experimental values to simulated CVs (Figure 3b,c). Using the experimentally determined diffusion coefficient of $D_o = 3.6 \times 10^{-6}$ $cm^2$ $s^{-1}$ for the cubane (see SI) and assuming a transfer coefficient of $\alpha = 0.5$,[33] values of $k$ were obtained by simulating CVs to produce the curves shown in Figure 3b, which best fit the experimental data points. By iterative variation of $k$, this procedure yielded rate constants with an estimated error of 10%. By varying the acidity of the medium, the $k$ for the PCET oxidation, $k_{PCET}$, of **1**-$H^+$ to **2** at pH 1 was found to be roughly an order of magnitude slower than the $k$ for simple ET oxidation, $k_{ET}$, of **1** to **2** at pH 4 (Figure 3b). Intriguingly, $k_{PCET}$ values for the oxidation of **1**-$H^+$ in both $H_2O$ and $D_2O$ at pH 1 and pD 1, respectively (Figure 3c), are similar. Absence of an observable kinetic isotope effect is consistent with a PCET mechanism that is stepwise under low pH conditions (where species **1**-$H^+$ is converted to deprotonated **2**).[34] Moreover, the observed decrease in $k_{PCET}$ at pH 1 relative to $k_{ET}$ at pH 4 is indicative of an equilibrium proton transfer followed by rate-limiting electron transfer (proton−electron transfer, PET) mechanism.[33,35]

To independently assess the role of the proton on the kinetics of electron transfer, we isolated cubane **2** (synthesized via oxidation of **1** by ceric ammonium nitrate)[32] and studied the rate of self-exchange (SE) in solutions containing **1** and **2** (pD 4) and **1**-$H^+$ and **2** (pD 1) in $D_2O/D_2SO_4$ by $^1$H NMR spectroscopy. In isolation, all three complexes were found to have a single set of sharp, well-defined $^1$H NMR signals, with only a moderate paramagnetic shift for the resonances of **2**, consistent with a high degree of delocalization of charge over the $Co_4O_4$ core.[32] Titration of solutions of **1**-$H^+$ with **2** at pD 1 in $D_2O/D_2SO_4$ with 1% DSS (2,2-dimethyl-2-silapentane-5-sulfonate, added as a control for nonexchange-related paramagnetic line broadening)[36] was observed to give only very minor signal broadening due to SE (Figure S1, Supporting Information [SI]). Fitting the observed signal broadening at varying concentrations of **2** with in silico-simulated spectra (Figure S1, SI) provided the $k_{obs}$ values shown in Figure 4a. For pD = 1, the slope of this line yields a second-order rate constant for SE to be $k_D$ = 13,000 ± 2,400 $M^{-1}$ $s^{-1}$. Variable-temperature NMR studies, shown in Figure S3 (SI), allowed values of $\Delta H^{\ddagger} = +35.2 \pm 1.3$ kJ $mol^{-1}$ and $\Delta S^{\ddagger} = -110 \pm 3$ J $K^{-1}$ $mol^{-1}$ to be determined from Eyring plots (Figure S4, SI), consistent with a high-energy transition state where two positively charged


dx.doi.org/10.1021/ja110908v | J. Am. Chem. Soc. 2011, 133, 5174–5177

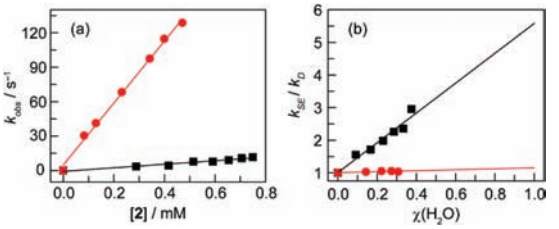


**Figure 4.** (a) Plot of population adjusted self-exchange rate constant, $k_{obs}$, vs concentration of the oxidized cubane, **2** for pD = 1 (■) and pD = 4 (red ●). (b) Plot of the second-order rate constant for self-exchange relative to that for self-exchange in all-deuterated solvent ($k_{SE}/k_D$) vs mole fraction of protonated solvent present ($\chi(H_2O)$) for pH/D = 1 (KIE = 4.3 ± 0.2) (■) and pH/D = 4 (KIE ≈ 0) (red ●).

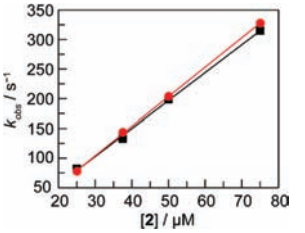


**Figure 5.** Pseudo-first-order rate constants for the oxidation of 5 μM [Ru(bpy)$_3$]Cl$_2$ by excess **2** measured in 0.1 M $H_2SO_4/H_2O$ (■) and 0.1 M $D_2SO_4/D_2O$ (red ●). Calculated second-order rate constants are $1.2 \times 10^6$ $M^{-1}$ $s^{-1}$ (0.1 M $H_2SO_4/H_2O$) and $1.3 \times 10^6$ $M^{-1}$ $s^{-1}$ (0.1 M $D_2SO_4/D_2O$).

species come into close contact and may be bridged by ordered solvent molecules hydrogen bonded to the redox partners. In contrast, titration of **2** into solutions of **1** at pD 4 in $D_2O/D_2SO_4$ gave marked increases in line width over the same range of concentrations (Figure S2, SI), evincing a roughly 20-fold rate increase on raising the pD from 1 to 4 ($k_{SE4}$ = 300,000 ± 21,000 $M^{-1}$ $s^{-1}$ at pD 4).

We next examined the SE process for **1**-$H^+$ and **2** in pD 1 $D_2O/D_2SO_4$ while adding varying amounts of a pH 1 solution of $H_2O/H_2SO_4$ (Figure 4b). Simulation of the resulting $^1$H NMR spectra, after correction for the decreasing concentration of **2**, yielded a linear dependence of the SE rate constant, $k_{SE}$, on the fractional amount of $H_2O/H_2SO_4$ ($\chi H_2O$) present. Extrapolation of this plot to $\chi H_2O = 1$ yields a kinetic isotope effect (KIE, $k_{SE}/k_D$) of 4.3 ± 0.2. This observation points to a concerted pathway at pH 1. This KIE is not apparent in the electrochemical rate constant measurements. If it were, then the trumpet plot of Figure 3c would be given by the dashed line for data collected in deuterated solvent. A value of KIE = 4.1 would correspond to a $k$ of 0.041 cm $s^{-1}$ for the electrochemical oxidation in the all-deuterated case. This further substantiates that a CPET pathway does not prevail when **1**-$H^+$ is oxidized at an electrode. Similar $^1$H NMR titrations at pH/D 4 did not give a noticeable KIE, consistent with the supposition that no proton (or deuteron) transfers during this simple ET reaction.

To rule out effects associated with the solid/solution interface, we examined the homogeneous *bidirectional* PCET reaction between oxidized cubane **2** and a one-electron transfer reagent, [Ru(bpy)$_3$]Cl$_2$ (bpy =2,2′-bipyridine) by stopped-flow spectroscopy. The redox potential for the $Ru^{II/III}$ couple in $[Ru(bpy)_3]^{2+}$ is +1.26 V,[37] indicating that the redox process for the conversion of **2** → **1**-$H^+$ by $Ru(bpy)_3^{2+}$ has ∼100 mV driving force at pH 1 (Figure 2). The strong decrease in the absorbance at 450 nm upon oxidation of $Ru^{II}$ to $Ru^{III}$ by **2** (Figure S7, SI, green to dashed pink lines) permits the bidirectional PCET reaction to be monitored by the stopped-flow spectrophotometer. Monoexponential decay traces were observed for all reactions as the concentration of **2** was varied over a range that ensured pseudo-first-order conditions. Figure S8 (SI) shows decay traces and the monoexponential fits to furnish $k_{obs}$. $k_{obs}$, as a function of the concentration of **2**, is displayed in Figure 5, where the slopes of the lines yield nearly identical second-order rate constants of $1.2 \times 10^6$ $M^{-1}$ $s^{-1}$ and $1.3 \times 10^6$ $M^{-1}$ $s^{-1}$ in pH 1 $H_2O/H_2SO_4$ and pD 1 $D_2O/D_2SO_4$, respectively. This observation indicates no KIE for the reduction of **2** to **1**-$H^+$ by $[Ru(bpy)_3]^{2+}$. As the ruthenium complex is incapable of accepting a proton in either its oxidized or reduced forms, this experiment corresponds to a homogeneous bidirectional PCET reaction with $H_3O^+$ acting as the proton donor to the cubane to furnish **1**-$H^+$. Absence of a KIE again suggests a stepwise PCET mechanism where ET is rate-limiting.

EPR and XAS studies establish that appreciable Co(IV) is formed at potentials sufficient for water oxidation. We expect the Co(III)/Co(IV) conversion to be critical to the function of Co-Pi. We turned to the cubane model to examine the Co(III)/Co(IV) conversion via three complementary equations

$$\mathbf{1}\text{-}H^+ + h^+ \rightleftharpoons \mathbf{2} + H^+ \quad (1)$$

$$\mathbf{2} + [Ru^{2+}] + H^+ \rightleftharpoons \mathbf{1}\text{-}H^+ + [Ru^{3+}] \quad (2)$$

$$\mathbf{1}\text{-}H^+ + \mathbf{2}^* \rightleftharpoons \mathbf{2} + \mathbf{1}^*\text{-}H^+ \quad (3)$$

This study reveals that eqs 1 and 2 proceed by stepwise PCET, but the SE eq 3 proceeds by concerted PCET. We can rationalize this change in mechanism by considering the energetic barriers to forming the reaction intermediates for the various competing pathways. We first note that a second plateau at low pH/high potential is not observed in the diagram in Figure 2, indicating that the p$K_a$ of **2**-$H^+$ is below 0 and that the potential for the proton-independent process, $E_{1/2}$(**2**-$H^+$/**1**-$H^+$) (upper plateau in Figure 6), must be >1.41 V. Thus, we expect **2**-$H^+$ to be the most unstable species among the possible intermediates, and avoiding its formation is a crucial determinant of the mechanism for Co(III)/Co(IV) PCET.

Stepwise pathways for eqs 1 and 2 that avoid the **2**-$H^+$ intermediate are as follows:

$$\mathbf{1}\text{-}H^+ + h^+ \rightleftharpoons \mathbf{1} + H^+ + h^+ \rightleftharpoons \mathbf{2} + H^+ \quad (4)$$

$$\mathbf{2} + [Ru^{2+}] + H^+ \rightleftharpoons \mathbf{1} + [Ru^{3+}] + H^+ \rightleftharpoons \mathbf{1}\text{-}H^+ + [Ru^{3+}] \quad (5)$$

For eq 4, the intermediates are energetically disfavored by the difference between $E^0$ = 1.36 V at pH = 1 (the pH at which eq 1 was examined) and the proton-independent couple, $E_{1/2}$(**2**/**1**) = 1.25 V (the lower plateau in Figure 2); this difference of 0.11 V is shown by Figure 6C. Similarly, for sequence 5, the intermediates are disfavored by the difference between $E_{1/2}(Ru^{II/III})$ = 1.26 V and $E_{1/2}$(**2**/**1**) 0.01 V (Figure 6B). Therefore, eqs 4 and 5 incur <0.11 V energy penalties by avoiding the high-energy **2**-$H^+$ species.

In contrast, the only stepwise pathway for the SE eq 3 that avoids the **2**-$H^+$ intermediate is the three-step sequence:

$$\mathbf{1}\text{-}H^+ + \mathbf{2}^* \rightleftharpoons \mathbf{1} + H^+ + \mathbf{2}^* \xrightarrow{k_{SE4}} \mathbf{2} + H^+ + \mathbf{1}^* \rightleftharpoons \mathbf{2} + \mathbf{1}^*\text{-}H^+ \quad (6)$$

where the SE rate, $v_{SE}$, is given by

$$v_{SE} = k_{SE4}[\mathbf{1}][\mathbf{2}] = k_{SE4}\frac{K_a}{[H^+]}[\mathbf{1}\text{-}H^+][\mathbf{2}] \quad (7)$$

$$k_{SE1} = k_{SE4}\frac{K_a}{[H^+]} \quad (8)$$

Using the ET rate constant for SE at pH 4, $k_{SE4}$, and the acid dissociation constant of **1**-$H^+$, $K_a$, the PCET rate constant for SE at


dx.doi.org/10.1021/ja110908v | J. Am. Chem. Soc. 2011, 133, 5174–5177

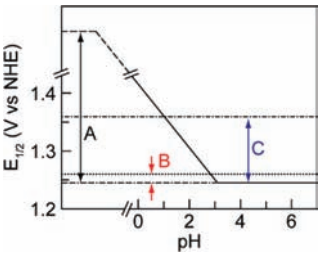


**Figure 6.** Schematic representation of the energetic penalties for forming intermediates in the stepwise PCET pathways. **A** PCET self-exchange; **B**, reduction by $[Ru(bpy)_3]Cl_2$; and **C**, the electrode reaction at pH 1. (**A** > 0.16, **B** = 0.01, **C** = 0.11 V). Dashed region of Pourbaix diagram represents hypothetical data. Horizontal lines denote the potential of the electrode at pH 1 (-·--·-), $[Ru(bpy)_3]^{2+/3+}$ couple (· · · ·), **1**/**2** couple (--·--·).

pH 1, $k_{SE1}$, is calculated to be 2400 $M^{-1}$ $s^{-1}$ for reaction 6. This rate constant for the *stepwise* mechanism in reaction 6 is smaller than the value observed for *concerted* SE at pH 1, 55,900 $M^{-1}$ $s^{-1}$ ($k_D$ × KIE), excluding the stepwise sequence as a viable alternative.

An alternative to the stepwise mechanism of eq 6, is to proceed through **2**-$H^+$ for the SE eq,

$$\mathbf{1}\text{-}H^+ + \mathbf{2}^* \rightleftharpoons \mathbf{1} + \mathbf{2}^*\text{-}H^+ \rightleftharpoons \mathbf{2} + \mathbf{1}^*\text{-}H^+ \qquad (9)$$

The intermediates are energetically disfavored by the difference between $E_{1/2}$(**2**-$H^+$/**1**-$H^+$) > 1.41 V and $E_{1/2}$(**2**/**1**) (Figure 6A) which is >0.16 V. We note that this is a lower limit for the ET/PT process. That the observed SE eq 3 exhibits a sizable KIE suggests that the SE proceeds by concerted PCET, owing to the energy barrier for forming a discrete **2**-$H^+$ species.

The foregoing analysis illustrates that the high-energy penalty for forming **2**-$H^+$ forces a concerted pathway for *unidirectional* PCET SE, whereas *bidirectional* PCET reactions, which can avoid forming **2**-$H^+$, proceed via stepwise pathways. With regard to Co-Pi water oxidation catalysis, the SE reaction provides a model for charge transfer through the film since we expect that the Co(III)/Co(IV) self-exchange reaction mediates conduction via electron hopping. The results reported herein extend the growing body of work demonstrating that concerted PCET[10,38−40] can avoid high-energy intermediates and thus suggest that PCET is not only important for the activation of water by Co-Pi but also plays a role in the propagation of charge through the catalyst film.

## ■ ASSOCIATED CONTENT

**Supporting Information.** This material is available free of charge via the Internet at http://pubs.acs.org.

## ■ AUTHOR INFORMATION

**Corresponding Author**
nocera@mit.edu

## ■ ACKNOWLEDGMENT

We are indebted to Prof. C. Costentin and Prof. J. Bonin (Université Paris-Diderot) for discussions. We thank Prof. S. Lippard and Dr. Christine Tinberg (MIT) for assistance with the stopped-flow studies and Arturo Pizano (MIT) for useful suggestions. Y.S. gratefully acknowledges the NSF for a predoctoral fellowship. D.A.L. gratefully acknowledges the Jane Coffin Childs Memorial Fund for Medicinal Research for a postdoctoral fellowship. This research was supported by AFOSR FA9550-09-1-0689 and a generous donation from the Chesonis Family Foundation.

## ■ REFERENCES

(1) Lewis, N. S.; Nocera, D. G. *Proc. Natl. Acad. Sci. U.S.A.* **2006**, *103*, 15729.
(2) Abbott, D. *Proc. IEEE* **2010**, *98*, 42.
(3) Hoffert, M. I.; Caldeira, K.; Jain, A. K.; Haites, E. F.; Harvey, L. D. D.; Potter, S. D.; Schlesinger, M. E.; Schneider, S. H.; Watts, R. G.; Wigley, T. M. L.; Wuebbles, D. J. *Nature* **1998**, *395*, 881.
(4) Smalley, R. E. *Mater. Res. Soc. Bull.* **2005**, *30*, 412.
(5) Nocera, D. G. *Inorg. Chem.* **2009**, *48*, 10001.
(6) Gust, D.; Moore, T. A.; Moore, A. L. *Acc. Chem. Res.* **2009**, *42*, 1890.
(7) Cook, T. R.; Dogutan, D. K.; Reece, S. Y.; Surendranath, Y.; Teets, T. S.; Nocera, D. G. *Chem. Rev.* **2010**, *110*, 6474.
(8) Huynh, M. H. V.; Meyer, T. J. *Chem. Rev.* **2007**, *107*, 5004.
(9) Hammes-Schiffer, S. *Acc. Chem. Res.* **2009**, *42*, 1881.
(10) Costentin, C. *Chem. Rev.* **2008**, *108*, 2145.
(11) Mayer, J. M. *Annu. Rev. Phys. Chem.* **2004**, *55*, 363.
(12) A Ni analogue has also been reported; see Dincă, M.; Surendranath, Y.; Nocera, D. G. *Proc. Natl. Acad. Sci. U.S.A.* **2010**, *107*, 10337.
(13) Kanan, M. W.; Nocera, D. G. *Science* **2008**, *321*, 1072.
(14) Surendranath, Y.; Dincă, M.; Nocera, D. G. *J. Am. Chem. Soc.* **2009**, *131*, 2615.
(15) Esswein, A. J.; Surendranath, Y.; Reece, S. R.; Nocera, D. G. *Energy Environ. Sci.* **2011**, *4*, 499.
(16) Lutterman, D. A.; Surendranath, Y.; Nocera, D. G. *J. Am. Chem. Soc.* **2009**, *131*, 3838.
(17) Zhong, D. K.; Sun, J.; Inumaru, H.; Gamelin, D. R. *J. Am. Chem. Soc.* **2009**, *131*, 6086.
(18) Zhong, D. K.; Gamelin, D. R. *J. Am. Chem. Soc.* **2010**, *132*, 4202.
(19) Steinmiller, E. M. P.; Choi, K. S. *Proc. Natl. Acad. Sci. U.S.A.* **2009**, *106*, 20633.
(20) Kanan, M. W.; Surendranath, Y.; Nocera, D. G. *Chem. Soc. Rev.* **2009**, *38*, 109.
(21) Risch, M.; Khare, V.; Zaharieva, I.; Gerencser, L.; Chernev, P.; Dau, H. *J. Am. Chem. Soc.* **2009**, *131*, 6936.
(22) Kanan, M. W.; Yano, J.; Surendranath, Y.; Dincă, M.; Yachandra, V. K.; Nocera, D. G. *J. Am. Chem. Soc.* **2010**, *132*, 13692.
(23) Barber, J. *Inorg. Chem.* **2008**, *47*, 1700.
(24) Takahashi, Y.; Gotoh, Y.; Akimoto, J. *J. Solid State Chem.* **2003**, *172*, 22.
(25) McAlpin, J. G.; Surendranath, Y.; Dincă, M.; Stich, T. A.; Stoian, S. A.; Casey, W. H.; Nocera, D. G.; Britt, R. D. *J. Am. Chem. Soc.* **2010**, *132*, 6882.
(26) Surendranath, Y.; Kanan, M. W.; Nocera, D. G. *J. Am. Chem. Soc.* **2010**, *132*, 16501.
(27) Bockris, J. O.; Otagawa, T. *J. Phys. Chem.* **1983**, *87*, 2960.
(28) Lyons, M. E. G.; Brandon, M. P. *Int. J. Electrochem. Sci.* **2008**, *3*, 1425.
(29) Singh, R. N.; Koenig, J.-F.; Poillerat, G.; Chartier, P. *J. Electrochem. Soc.* **1990**, *137*, 1408.
(30) Dimitrou, K.; Folting, K.; Streib, W. E.; Christou, G. *J. Am. Chem. Soc.* **1993**, *115*, 6432.
(31) Dimitrou, K.; Brown, A. D.; Folting, K.; Christou, G. *Inorg. Chem.* **1999**, *38*, 1834.
(32) Dimitrou, K.; Brown, A. D.; Concolino, T. E.; Rheingold, A. L.; Christou, G. *Chem. Commun.* **2001**, 1284.
(33) Costentin, C.; Robert, M.; Savéant, J.-M.; Teillout, A.-L. *Proc. Natl. Acad. Sci. U.S.A.* **2009**, *106*, 11829.
(34) Costentin, C.; Louault, C.; Robert, M.; Savéant, J.-M. *Proc. Natl. Acad. Sci. U.S.A.* **2009**, *106*, 18143.
(35) Costentin, C.; Robert, M.; Savéant, J.-M.; Teillout, A.-L. *ChemPhysChem* **2009**, *10*, 191.
(36) Beattie, J. K.; Elsbernd, H. *Inorg. Chim. Acta* **1995**, *240*, 641.
(37) Creutz, C.; Sutin, N. *Inorg. Chem.* **1976**, *15*, 496.
(38) Sjödin, M.; Ghanem, R.; Polivka, T.; Pan, J.; Styring, S.; Sun, L.; Sundström, V.; Hammarström, L. *Phys. Chem. Chem. Phys.* **2004**, *6*, 4851.
(39) Irebo, T.; Reece, S. Y.; Sjödin, M.; Nocera, D. G.; Hammarström, L. *J. Am. Chem. Soc.* **2007**, *129*, 15462.
(40) Bonin, J.; Costentin, C.; Louault, C.; Robert, M.; Routier, M.; Savéant, J.-M. *Proc. Natl. Acad. Sci. U.S.A.* **2010**, *107*, 3367.